Emergent percolation length and localization in random elastic networks

Ariel Amir*,[1] Jacob J. Krich*,[2, 3] Vincenzo Vitelli,[4] Yuval Oreg,[5] and Yoseph Imry[5]

[1]*Department of Physics, Harvard University, Cambridge, MA 02138, USA*
[2]*Department of Physics, University of Ottawa, Ottawa, ON, Canada*
[3]*Department of Chemistry and Chemical Biology,*
Harvard University, Cambridge, Massachusetts 02138, USA
[4]*Instituut-Lorentz for Theoretical Physics, Leiden University, Leiden NL 2333 CA, The Netherlands*
[5]*Department of Condensed Matter Physics, Weizmann Institute of Science, Rehovot, 76100, Israel*

We study, theoretically and numerically, a minimal model for phonons in a disordered system that shows rich behavior in the localization properties of the phonons as a function of the density, frequency and the spatial dimension. We use a percolation analysis to argue for a Debye spectrum at low frequencies for dimensions higher than one, and for a localization/delocalization transition. We show that in contrast to the behavior in electronic systems, the transition exists for arbitrarily large disorder, albeit with an exponentially small critical frequency. The structure of the modes reflects a divergent percolation length that arises from the disorder in the springs without being explicitly present in the definition of our model. We calculate the speed-of-sound of the delocalized modes (phonons) and corroborate it with numerics. We calculate the critical frequency of the localization transition at a given density and test the prediction numerically using a recursive Green function method.

Despite decades of experimental and theoretical efforts, the mechanical properties of disordered solids remain poorly understood. Long-standing challenges in materials science such as explaining the low-temperature properties of glasses and ultrasound propagation in granular media require a robust understanding of the effect of disorder on vibrational modes and their localization properties. Interest in phonon localization in disordered solids has been rekindled by recent experiments on colloidal glasses that mimic several vibrational properties of molecular glasses on larger length and time scales [1–3]. A significant advantage of colloidal glasses is that their vibrational modes can be experimentally reconstructed, and they are found to exhibit fascinating localization properties.

Since Anderson's seminal work [5], the localization of electronic wave-functions in disordered metals has been the subject of several successful theoretical investigations [6]. The study of the vibrational modes of a disordered network of masses and springs (see Fig. 1), which is analogous to the electronic problem, received significantly less attention. Previous approaches to study this problem include perturbative analysis [7] that applies to weakly disordered solids, transfer matrix techniques that are restricted to one dimension [8–10], numerical studies [11–16] and renormalization group approaches [3, 17, 18, 20]. One of the successful approaches to modeling vibrations in disordered systems has been using the framework of Euclidean random matrices [7, 21–29]. This problem is mathematically related to the localization problem on sparse graphs [30–33], to the problem of a random walker in a disordered environment [3, 34, 35], and was also used to explain aging and slow relaxations in electron glasses [36–38].
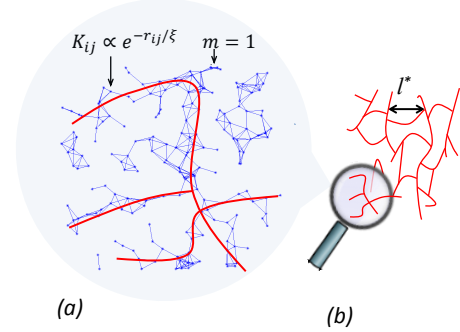

FIG. 1. (a) A schematic example of a network of springs and masses. All masses are identical with value arbitrarily chosen as unity, while the springs are broadly distributed and their value is exponential in the Euclidean distance between each pair of masses. In the figure, only springs with a strength exceeding a threshold K_{opt} are shown, see Eq. (1) of the SM. (b) A sketch of the percolating network, yielding a meshwork of pathways, and its characteristic length scale l^* [4]. We will show that for system size $L \gg l^*$, and for dimensions $d > 1$, one can effectively describe the low-lying modes using continuum elasticity, leading to a Debye spectrum.

Many important questions still remain open regarding the nature of the localization transition of the vibrational modes in disordered systems, its dependence on the dimensionality and the type of the disorder (non-uniform masses versus non-uniform springs), and amorphous materials such as colloidal glasses still pose many theoretical challenges. Most studies rely on numerical solutions, or study a particular asymptotic limit, and analytic solutions for tunable disorder and system dimensionality are scarce. In this work, we present a model that is analytically tractable, leading to insights into the way the localization transition depends on the disorder magni-

tude and dimensionality, and elucidating the emergence of a disorder-dependent length scale which determines various elastic properties of the system.

Continuum elastic theories of disordered solids typically break down below a mesoscopic length scale ℓ^* (controlled by the amount of disorder) intermediate between particle diameter and system size [39–41]. In jammed packings of grains and random networks, ℓ^* exhibits a power law divergence whenever the network connectivity or packing density are lowered towards the critical values necessary to hold these systems rigid. At low densities (weak connectivity) the effect of disorder is stronger. Plane-wave vibrational modes, which satisy the Deybe density of states, exist only below a critical frequency $\omega^* \sim 1/\ell^*$ that goes to zero at the critical point.

In the following, we present a minimal model for a random elastic network, which we treat analytically using percolation theory. We find that above two dimensions there is always a localization transition at finite frequency, for arbitrarily large disorder. We find an approximate analytical expression for the critical frequency, which we verify numerically using a recursive Green function and finite-size scaling technique. For the delocalized modes, we calculate, analytically and numerically, the speed-of-sound, which is directly related to the low-frequency spectrum. The mesoscopic length scale ℓ^* emerges naturally from the percolation picture, and plays a significant role in the calculation of the speed-of-sound and the phase diagram.

The model.- Our model of the vibrational properties of disordered solids is schematically illustrated in Fig. 1a, which shows point particles (with equal masses, $m = 1$) randomly and uniformly distributed in a d-dimensional space, with average nearest-neighbor distance r_{nn}. Between every pair of points $\{i,j\}$ there is a spring with spring constant K_{ij}. We choose:

$$K_{ij} = \frac{U}{\xi^2} e^{-r_{ij}/\xi}, \ K_{ii} = -m \sum_{j \neq i} K_{ij}, \qquad (1)$$

where r_{ij} is the distance between particles i and j, U is a characteristic energy scale and ξ is the range of the exponential interaction. The vibrational frequencies ω_i are related to the eigenvalues λ_i of the $N \times N$ matrix K, as $\omega_i^2 = -\lambda_i$. This model describes scalar elasticity, *i.e.*, it neglects the vectorial nature of the forces [3, 21]. The randomly chosen points represent the equilibrium locations for the masses. In our simple model it is the dimensionless ratio $\epsilon \equiv \xi/r_{nn}$ that controls the strength of the disorder – the low density limit ($\epsilon \ll 1$) corresponds to strong disorder. The sum of every row and column of K vanishes, due to the negative diagonal elements. This 'sum-rule' is a result of momentum conservation in the problem, which has important consequences for the localization properties and the resulting vibrational spectrum [42, 43]. This sum-rule is associated with a purely

delocalized mode with $\omega = 0$, corresponding to a uniform translation of all masses. The vibrational problem is mathematically equivalent to that of a classical random walker in a disordered landscape [35, 44]; for the diffusion problem K describes the Markov process, and the probability of being on site j satisfies $\dot{p}_j = K_{ji}p_i$; the sum-rule now enforces probability conservation.

It is not obvious a priori whether the low-frequency vibrational modes of this system are localized. It was previously shown that the states with $\omega > \omega^*$ are localized, with $\omega^* \to 0$ at low density [3]. However, since there is always a delocalized mode at $\omega = 0$, from continuity one might expect that in a large enough system, modes of sufficiently low frequency would also be delocalized. We find that this is indeed the case above two dimensions. Another, perhaps simpler, question regards the structure of the density-of-states (DOS) of the eigenvalue distribution at low frequencies [45]. Will it be the same as that of an ordered system, manifesting a Debye spectrum, $P(\omega) \sim \frac{\omega^{d-1}}{c^d}$ (with c the speed-of-sound), or can the disorder change it qualitatively? One may think that a Debye spectrum and delocalized modes should go hand-in-hand, but we shall shortly give a counter-example in a one-dimensional system. In dimensions higher than one, however, we will show that one always obtains a Debye spectrum at sufficiently low frequencies.

In one dimension and at low densities, the model we study reduces to a chain of equal masses connected by random springs. For low densities we can neglect matrix elements beyond nearest-neighbors, and obtain a power-law distribution of the remaining ones [9, 10]. For sufficiently small disorder (corresponding to large enough ϵ) one obtains a Van-Hove singularity of $P(\omega) = const$ at small eigenvalues, which is Debye-like, while for densities lower than the critical density $\epsilon = 1$ a sharper power law $P(\omega) \propto 1/\omega^\alpha$ occurs, with $0 < \alpha < 1$. In the one-dimensional case, all the eigenmodes are localized for any density, with the localization length diverging as $\omega \to 0$. The fact that the spectrum can still be Debye-like for $\epsilon > 1$ shows that one can have localized states and Debye simultaneously. Note, however, that at high densities the nearest-neighbor model and the one discussed here do not match, since in our case far neighbors will also be important. We now proceed to analyze the model in higher dimensions, treating separately the cases of high and low densities.

Structure of the eigenmodes at low density.- A key step in our approach is to realize that the vibrational properties of this spring network can be effectively described in terms of an emergent percolation network (shown schematically in Fig. 1b) constructed by retaining only springs with $K_{ij} > K_{opt}$. The optimal spring constant K_{opt} will be shown to be proportional to the critical spring constant K_c, which is defined to be the maximal spring constant such that all the springs in the system with values greater than K_c form an infinite percolat-

ing cluster. If we retain only the springs in the infinite cluster, the spring network will span the system, but will nevertheless have an infinite compressibility (resistivity in the analogous electronic problem), since a macroscopic load will have to be held by a single 'bottle-neck' spring. If, on the other hand, we retain all springs larger than K, with $K < K_c$, we will obtain not a single percolating path, but a grid of such paths, with a typical mesh size of order l^*, see Fig. 1b.

The value of K_{opt} can be found by optimizing the compressiblity, as shown in the Supplementary Material (SM), leading to $K_{opt} = K_c e^{-\nu(d-2)}$. This construction is made with complete analogy to the electronic system [4], with inverse compressibility playing the role of conductivity. The percolation length l^* signals the scale below which continuum elasticity breaks-down, and the scale above which fluctuations in the compressibility become relatively small [4]. As described in the SM, $l^* \sim 1/\epsilon^\nu$, and thus it diverges for low densities.

We can 'coarse-grain' the sparse percolation network of masses and springs, over a length scale of the order of the percolation correlation length l^*, as illustrated in Fig. 1. Since $K(r)$ decays exponentially, the effective spring constant of each coarse-grained box can be approximated by the optimal spring K_{opt} with all other springs effectively stiff ($K \gg K_{opt}$) or broken ($K \ll K_{opt}$) [4]. By coarse-graining over regions of order l^*, the resulting distribution of critical springs will be narrow, and we have essentially replaced the disordered spring network by an approximately ordered one; the fluctuations in the values of the spring constants have been suppressed by the coarse-graining procedure. Note that the topology of this network is ordered by construction, since we coarse-grained over boxes. This reasoning suggests that locally, the spatial structure of the low-energy eigenmodes should coincide with that of the percolating network, but that the coarse-grained network would support plane-wave, delocalized modes, as would a perfectly ordered system. This procedure is only defined in dimensions greater than one, where percolation occurs.

Using the coarse-graining construction we replaced the system by an ordered one, and thus we can readily find the speed-of-sound of the delocalized modes at low densities: $c = \sqrt{K_{opt}/ml^*}$, where m is the effective mass of each coarse-grained oscillator, and the critical spring constant K_c can be found from continuum percolation theory[4]; namely, $K_c \sim e^{-P_d/\epsilon}$, with $P_d = 2(\eta_c/V_d)^{1/d}$, where V_d is the volume of the d-dimensional unit sphere and η_c is the standard continuum percolation threshold [47, 48], giving $P_2 = 1.20$ and $P_3 = 0.87$. As previously discussed $l^* \sim \frac{1}{\epsilon^\nu}$, with the critical exponent ν equal to 4/3 in 2D [49]. The fractal dimension of the percolating cluster D_p is smaller than the system dimensionality d, and is approximately 1.9 in 2D and 2.5 in 3D [50]. Since the size of each coarse-grained box is comparable to l^{*d}, we expect the total mass of each block to scale as
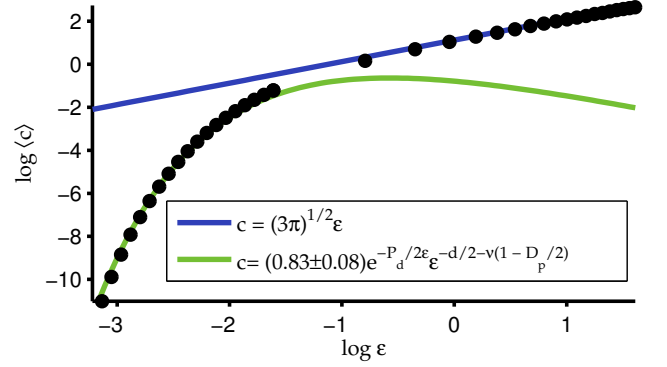

FIG. 2. The speed of sound of the low frequency delocalized modes as a function of the density parameter ϵ, for a two-dimensional system. A low value of ϵ corresponds to a highly disordered, sparse network, where the distribution of spring constants is very broad. The energy scale $U = 1$, see Eq. (1), and $r_{nn} = 1$. The straight line shows the exact prediction at high densities, below Eq. (4). The other line shows the prediction of Eq. (2) of an exponentially suppressed speed at low densities, as predicted from percolation theory, taking the prefactor as a fitting parameter. The value of P_d depends on the system dimensionality, and it is equal to 1.20 in two dimensions [48], in good agreement with the numerical results.

$m \sim \epsilon^d l^{*D_p} \sim \epsilon^{d-\nu D_p}$. Combining these results for l^*, m and K_{opt} gives:

$$c \sim e^{-\frac{P_d}{2\epsilon}} \epsilon^{-[d/2+\nu(1-D_p/2)]}. \tag{2}$$

This form is corroborated numerically in 2d in Fig. 2, comparing the exact diagonalization of large matrices. For each $\epsilon \leq 0.2$, we determined c by averaging results from 2000 realizations with $N = 20000$ sites with free boundary conditions. For each $\epsilon > 0.2$ we used a single realization with $N = 10000$. For each matrix, the low-lying eigenvectors were determined. We discarded the uniform mode and Lifshitz modes [5], where a small number of sites are isolated from their neighbors. The smallest remaining eigenvalue $-\omega_0^2$ gave $c = L\omega_0/\pi$, where the system has linear size $L = N^{1/d}/\epsilon$, with $\xi = 1$. For ϵ from 0.2 to 0.044, the standard deviation in values of c ranged from 1% to 30% of the mean, respectively. The value shown in Fig. 2 was well determined, with statistical error smaller than the symbol size. The SM shows further results that the degeneracies of the low-lying eigenvalues match what is expected from plane waves in an ordered box geometry, see Table S1. Moreover, Fig. 1 in the SM shows the average spatial profile of these low frequency modes, which is a plane-wave.

Following the same reasoning as the standard one for ordered systems, the DOS which follows from these plane-wave-like modes will be a Debye spectrum, and at low frequencies we find that: $P(\omega) \sim \frac{\omega^{d-1}}{c^d}$. In the SMs we give an alternative derivation for the form of the DOS at low frequencies, which relies on mapping this problem

to the diffusion problem of a classical random walker in a random landscape. Since the prefactor of the Deybe DOS depends on the speed-of-sound, this mapping also provides an additional way to find the exponential dependence of c on $1/\epsilon$, consistent with Eq. (2).

The delocalized plane-wave modes should cease to exist as their wavelength approaches the coarse-graining scale l^*, so we can estimate the delocalization transition frequency

$$\omega^* = ck^* \approx \frac{c}{l^*} = e^{-\frac{P_d}{2\epsilon}} \epsilon^{\nu D_p/2 - d/2}. \tag{3}$$

We have used a recursive Green function and finite-size scaling technique to systematically investigate whether states are localized or delocalized in the infinite-size system [6, 9], with results shown in Fig. 3. We adapted the technique from the one used in Ref. 54, which studied the same system without the diagonal terms of K. See the SM for details. The percolation prediction of Eq. 3 indicates that the delocalized modes should persist to arbitrarily small ϵ. Due to numerical precision limitations, we cannot study $\epsilon \leq 0.05$ in three dimensions and thus cannot numerically determine if there is a smaller ϵ at which all states are localized. The prediction of Eq. 3 is in good agreement with the numerically determined boundary, as shown in Fig. 3, for both two and three dimensions. The numerical results for 2d also seem to suggest a phase transition, in contrast to the behavior of electronic systems, where it is known that arbitrary small fluctuations will lead to localization in the orthogonal ensemble (which is the appropriate ensemble considering the symmetries of our problem). Further numerical and analytical study is needed, however, in order to firmly establish the existence of delocalized eigenmodes in $d = 2$.

High density.- For $\epsilon \gg 1$, the behavior is reminiscent of ordered systems: one can show that plane waves are approximate solutions to the eigenvalue problem [21] for $|\vec{k}|r_{nn} \ll 1$ and $\epsilon \gg 1$, where k is the wavevector. It is found that:

$$\lambda \approx \left(\frac{\epsilon}{\xi}\right)^d \int d\vec{r} K(\vec{r})[e^{i\vec{k}\cdot\vec{r}} - 1]. \tag{4}$$

If we denote the d-dimensional Fourier transform of $K(r)$ by $\hat{K}(\vec{k})$, this leads to [21]: $\lambda = -\omega^2 = \left(\frac{\epsilon}{\xi}\right)^d [\hat{K}(k) - \hat{K}(0)]$. For $K(r)$ decaying exponentially as in Eq. (1), in two dimensions, we find for $k\xi \ll 1$ acoustic phonons with a well-defined speed of sound $c = \frac{d\omega}{dk} = \sqrt{3\pi\epsilon^2 U}$. Fig. 2 shows the good agreement of this prediction with the result of exact diagonalization. In 3D, this argument produces acoustic phonons at small k, with $c^2 = 16\pi U \epsilon^3$.

Summary.- We have studied the vibrational spectrum of a disordered system, using analytical arguments relying on percolation theory and a coarse-graining RG-type
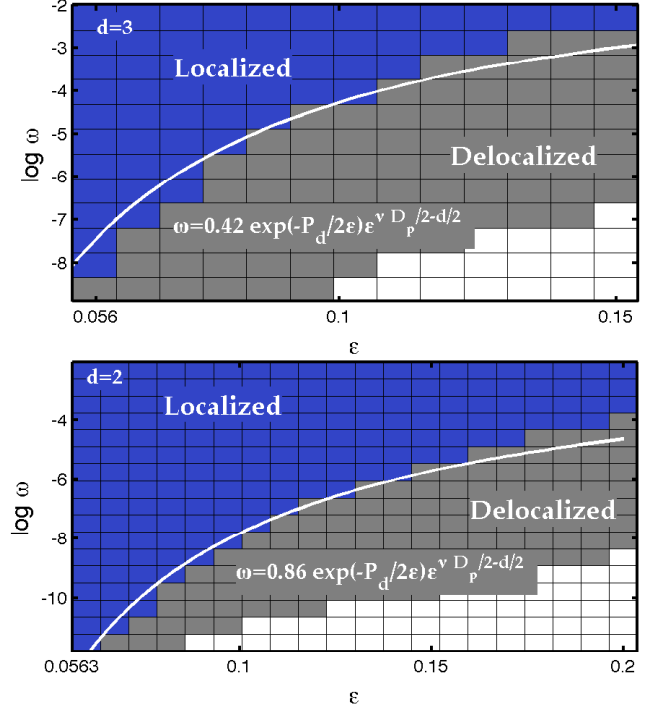

FIG. 3. Phase diagram showing the localized and delocalized modes dependence on density (ϵ) and frequency in two and three dimensions. As predicted in Eq. 3, there are both localized and delocalized modes at any density, and at low densities the critical frequency ω^* below which modes are delocalized depends on ϵ according to Eq. 3. The only fitting parameter in each line is the prefactor, which is found to be of order unity. White squares indicate parameters where states are so strongly delocalized that numerical results did not converge; see SM.

analysis, numerically exact diagonalization, and finite-size scaling. We find that for $d > 1$, there is a critical frequency ω^* vanishing with density, below which a Deybe DOS is observed. This frequency marks a localization-delocalization transition of the vibrational modes, which we study numerically in two and three dimensions. In two dimensions further studies are needed in order to ascertain whether this is a true phase transition. We analytically account for the speed-of-sound of the delocalized modes, both for the low and high density regimes, using a percolation approach. A lengthscale l^* emerges, which affects the speed-of-sound and the phase transition. In the future, it would be interesting to study the heat transport in these systems, and to compare the results of the minimal model presented here with those of amorphous solids.

* These authors contributed equally to this work.

———————

[1] A. Ghosh, V. K. Chikkadi, P. Schall, J. Kurchan, and D. Bonn, Phys. Rev. Lett. **104**, 248305 (2010).
[2] K. Chen, W. G. Ellenbroek, Z. Zhang, D. T. N. Chen, P. J. Yunker, S. Henkes, C. Brito, O. Dauchot, W. van Saarloos, A. J. Liu, and A. G. Yodh, Phys. Rev. Lett. **105**, 025501 (2010).
[3] D. Kaya, N. L. Green, C. E. Maloney, and M. F. Islam, Science **329**, 656 (2010).
[4] B. Shklovskii and A. Efros, *Electronic properties of doped semiconductors* (Springer-Verlag, Berlin, 1984).
[5] P. W. Anderson, Phys. Rev. **109**, 1492 (1958).
[6] Abrahams, E. (ed.): 50 Years of Anderson Localization. World Scientific, Singapore (2010).
[7] T. S. Grigera, V. Martin-Mayor, G. Parisi, P. Urbani, and P. Verrocchio, J. Stat. Mech. **2011**, P02015 (2011).
[8] F. J. Dyson, Phys. Rev. **92**, 1331 (1953).
[9] S. Alexander, J. Bernasconi, W. R. Schneider, and R. Orbach, Rev. Mod. Phys. **53**, 175 (1981).
[10] T. A. L. Ziman, Phys. Rev. Lett **49**, 337 (1982).
[11] S. I. Simdyankin, S. N. Taraskin, M. Elenius, S. R. Elliott, and M. Dzugutov, Phys. Rev. B **65**, 104302 (2002).
[12] S. D. Pinski, W. Schirmacher, and R. A. Römer, EPL (Europhysics Letters) **97**, 16007 (2012).
[13] B. J. Huang and T.-M. Wu, Phys. Rev. E **79**, 041105 (2009).
[14] V. I. Clapa, T. Kottos, and F. W. Starr, J. Chem. Phys. **136**, 144504 (2012).
[15] V. Vitelli, N. Xu, M. Wyart, A. J. Liu, and S. R. Nagel, Phys. Rev. E **81**, 021301 (2010).
[16] S. Ciliberti and T. S. Grigera, Phys. Rev. E **70**, 061502 (2004).
[17] S. John, H. Sompolinsky, and M. J. Stephen, Phys. Rev. B **27**, 5592 (1983).
[18] M. B. Hastings, Phys. Rev. Lett. **90**, 148702 (2003).
[3] A. Amir, Y. Oreg, and Y. Imry, Phys. Rev. Lett. **105**, 070601 (2010).
[20] C. Monthus and T. Garel, Journal of Physics A: Mathematical and Theoretical **44**, 085001 (2011).
[21] M. Mezard, G. Parisi, and A. Zee, Nuclear Physics B **3**, 689 (1999).
[22] C. R. Offer and B. D. Simons, Journal of Physics A: Mathematical and General **33**, 7567 (2000).
[23] E. Bogomolny, O. Bohigas, and C. Schmit, J. Phys. A **36**, 3595 (2003).
[24] G. Parisi, The European Physical Journal E: Soft Matter and Biological Physics **9**, 213 (2002), 10.1140/epje/i2002-10088-x.
[25] T. S. Grigera, V. Martín-Mayor, G. Parisi, and P. Verrocchio, Journal of Physics: Condensed Matter **14**, 2167 (2002).
[26] T. S. Grigera, V. Martín-Mayor, G. Parisi, and P. Verrocchio, Philosophical Magazine Part B **82**, 637 (2002).
[27] S. Ciliberti, T. S. Grigera, V. Martín-Mayor, G. Parisi, and P. Verrocchio, Phys. Rev. B **71**, 153104 (2005).
[28] S. E. Skipetrov and A. Goetschy, Journal of Physics A: Mathematical and Theoretical **44**, 065102 (2011).
[29] C. Ganter and W. Schirmacher, Phys. Rev. B **82**, 094205 (2010).
[30] F. L. Metz, I. Neri, and D. Bollé, Phys. Rev. E **82**, 031135 (2010).
[31] T. Aspelmeier and A. Zippelius, J. Stat. Phys. **144**, 759773 (2011).
[32] D. S. Dean, J. Phys. A **35**, L153 (2002).
[33] J. Stäring, B. Mehlig, Y. V. Fyodorov, and J. M. Luck, Phys. Rev. E **67**, 047101 (2003).
[34] H. Scher and E. W. Montroll, Phys. Rev. B **12**, 2455 (1975).
[35] W. Schirmacher and M. Wagener, Phil. Mag. B **65** 4, 607 (1992).
[36] A. Amir, Y. Oreg, and Y. Imry, Phys. Rev. B **77**, 165207 (2008).
[37] A. Amir, Y. Oreg, and Y. Imry, Phys. Rev. Lett. **103**, 126403 (2009).
[38] A. Amir, Y. Oreg, and Y. Imry, Annu. Rev. Condens. Matter Phys. **2**, 235 (2011).
[39] M. Wyart, Ann. Phys. (Paris) **30**, 1 (2005).
[40] A. J. Liu and S. R. Nagel, Ann. Rev. Cond. Matt. Phys. **1**, 347 (2010).
[41] M. van Hecke, J. Phys. Cond. Mat. **22**, 033101 (2010).
[42] Y. Beltukov and D. Parshin, JETP Lett. **93**, 598 (2011).
[43] C. Brito, G. Parisi and F. Zamponi, *Pinned particles stabilize the soft modes of a nearly jammed system*, arXiv:1205.6007.
[44] S. Reuveni, R. Granek, and J. Klafter, Phys. Rev. E **81**, 040103 (2010).
[45] Y. de Leeuw and D. Cohen, *Diffusion in sparse networks: linear to semi-linear crossover*, arXiv:1206.2495.
[4] V. Ambegaokar, B. I. Halperin, and J. S. Langer, Phys. Rev. B **4**, 2612 (1971).
[47] C. D. Lorenz and R. M. Ziff, J. Chem. Phys. **114**, 3659 (2001).
[48] J. A. Quintanilla and R. M. Ziff, Phys. Rev. E **76**, 051115 (2007).
[49] S. Smirnov and W. Werner, Mathematical Research Letters **8**, 729 (2001).
[50] M. B. Isichenko, Rev. Mod. Phys. **64**, 961 (1992).
[5] I. Lifshitz, Advances in Physics **13**, 483 (1964).
[6] A. MacKinnon and B. Kramer, Phys. Rev. Lett. **47**, 1546 (1981).
[9] P. Markos, Acta Physica Slovaca **56**, 561 (2006).
[54] J. J. Krich and A. Aspuru-Guzik, Phys. Rev. Lett. **106**, 156405 (2011).

Supplementary Material

FINDING THE OPTIMAL SPRING CONSTANT K_{opt} AND THE COMPRESSIBILITY

We denote by K_c the value of the critical spring associated with percolation, *i.e.*, it is the largest value possible for which springs with spring constants larger than K_c percolate through the infinite system. As described in the main text (and illustrated in Fig. 1), we retain all springs with spring constant larger than some value K, with $K < K_c$. This will lead to a a grid of such paths, with a typical mesh size of order l^*, see Fig. 1b of the main text. From percolation theory $l^* \sim (r - r_c)^{-\nu}$, with r and r_c the distances associated with the springs K and K_c. As in the analogous electronic problem (where resistivity replaces compressibility), this will lead to an inverse compressibility $\kappa^{-1} \sim K/l^{*d-2}$ (this can be seen by replacing the system by an ordered grid with lattice spacing l^* and the spring constant of each edge in the lattice is K). In our problem $r = \xi \log(K)$, and thus for a given choice of K the associated compressiblity is:

$$\kappa^{-1} \sim K[\xi \log(K/K_c)]^{\nu}. \tag{1}$$

As expected, the inverse compressibility vanishes at K_c, and thus clearly there is a maximal compressibility for some $K_{opt} < K_c$. A straightforward calculation gives:

$$K_{opt} = K_c e^{-\nu(d-2)}. \tag{2}$$

Since $K_{opt} \propto K_c$, the scaling of l^* is still $l^* \sim 1/\epsilon^{\nu}$. For low densities (small ϵ), corresponding to high disorder, this length scale diverges.

This leads to an inverse compressibility of:

$$\kappa^{-1} \propto K_c \epsilon^{\nu(d-2)}. \tag{3}$$

The polynomial correction term $\epsilon^{\nu(d-2)}$ of the inverse compressibility is consistent with the renormalization group results on a related model [1, 2], which suggest that the results are robust to the precise details of the disorder used.

DENSITY-OF-STATES AT LOW FREQUENCIES

We argue that the density-of-states will correspond to a Debye spectrum at low enough frequencies and for $d > 1$, for arbitrarily small ϵ. To show this, it will be useful to employ the mapping between the vibrational problem studied here and that of the classical random walker, discussed in the main text. For the diffusion problem, the return probability $R_i(t)$ is defined as the probability to be at site i at time t giving that we were at site i at time $t = 0$. It can be shown that [3] $R(t) \equiv \overline{R_i(t)} = \int P(\lambda)e^{-\lambda t}d\lambda$, where $R(t)$ is the average over all sites i, and $P(\lambda)$ is the density of states of the matrix K. This formula implies that a higher DOS at small frequencies corresponds to a larger return probability at long times, which suggests slower diffusion. In general, a Debye spectrum (in any dimension) corresponds to the case of normal diffusion and the return probability scales as $1/Dt^{d/2}$. Thus, to establish the existence of a Debye spectrum at low frequencies, it suffices to prove that at asymptotically long times a particle will undergo normal diffusion.

To perform this step, we employ another mapping, between random walks and electrical networks. Consider a random resistor network whose resistance between two sites is proportional to the matrix elements of K_{ij}, *i.e.*, the hopping rate. Then, the Einstein relation tells us that the diffusion coefficient of the network (if it is non-zero) will be proportional to the conductivity. Therefore, the question of establishing normal diffusion is equivalent to proving that a finite conductivity exists in the network. This result was proved using percolation methods [4], in an identical system where the matrix elements (resistors) between two sites depend on both their energy difference and distance. For the case of very high (infinite) temperature, the matrix elements depend only on the distance, exponentially, as in the case we discuss here. Thus, for dimensions higher than one, the result of Ref. 4 shows that there is conductivity, and therefore diffusion, at asymptotic times. Moreover, this allows us to derive the diffusion coefficient, since percolation theory gives the dependence of the conductivity on ϵ: $\sigma \propto D \propto e^{-P_d/\epsilon}$ [4].

We now explain how this relates to the results of Ref. [3], where a strong peak was shown to occur in the DOS at very small frequencies. There, it was shown that for low densities the DOS can be approximated by:

$$P(\omega) = \frac{dV_d e^{-\frac{V_d}{2}[\log(\omega^2/2)]^d}[\log(\omega^2/2)]^{d-1}}{\omega}. \tag{4}$$

where V_d is the volume of the d-dimensional sphere.

At low frequencies Eq. (4) does not conform to the Debye spectrum, giving a more-rapid decay. Thus Eq. (4) must fail near some frequency ω^*, which should approximately occur at the delocalization transition. Eq. (4) was derived by approximately calculating all moments of the eigenvalue distribution to an accuracy of $O(\epsilon^m)$ with $m > 1$. The critical frequency ω^* of Eq. (3) in the main text is small enough such that the corrections due to the Debye spectrum at low frequencies do not significant change any of the moments. Moreover, we can use

the form of ω^* to calculate the integral of the density-of-states described by Eq. (4), from ω^* to the upper cutoff $\omega^2 = 2$, corresponding to a pair of masses [3]. The result it that there is *always* a finite fraction of localized modes. Taking the Debye spectrum below ω^*, $P(\omega) \sim \frac{\omega^{d-1}}{c^d}$, and using the value of c from Eq. (2) of the main text, we can estimate the number of delocalized modes, and find that it scales as $\epsilon^{\nu d}$. As one goes to higher disorder (lower ϵ) the fraction of delocalized modes decreases, becoming negligible at large disorder.

Index	ω, 2D ord.	ω, 2D num.	ω, 3d ord.	ω, 3d num.
1	1	1	1	1
2	1	1.022	1	1.014
3	$\sqrt{2}$	1.415	1	1.033
4	2	1.994	$\sqrt{2}$	1.390
5	2	2.004	$\sqrt{2}$	1.397
6	$\sqrt{5}$	2.222	$\sqrt{2}$	1.426
7	$\sqrt{5}$	2.244	$\sqrt{3}$	1.678
8	$\sqrt{8}$	2.826	2	1.950
9	3	3.001	2	1.991
10	3	3.042	2	2.037

TABLE I. Comparison of the frequencies of the low lying modes of the perfectly ordered case (ord.) and the numerical results (num.) on the disordered case in 2d and 3d, for open boundary conditions. The first non-trivial frequency is normalized to 1. For the two-dimensional case N=500,000, and for the three-dimensional case for N=100,000, with $\epsilon = 0.1$.

NUMERICAL VERIFICATION OF DELOCALIZED MODES

We have tested the analytic arguments numerically, working with large, sparse matrices, obtained by truncating the full matrices: all elements smaller than a cutoff value are set to zero. For a small enough cutoff value the results are independent of the value of the cutoff, as they should be.

Some of the low-lying eigenmodes consist of Lifshitz-like, rare isolated points [5]. Their participation ratio is close to unity, and thus they are essentially localized on a single point, with a vanishingly small frequency, exponentially small in the distance separating this point from others. However, the contribution of these events to the density-of-states is negligible for a large enough system and for small enough frequencies, since it goes to zero faster than any power-law (note that this relies on the exponential decay of the matrix elements, and for other forms decaying faster with the distance this assertion might be false). Aside from the rare Lifshitz singularities, the low frequency modes are found to be delocalized in these finite systems in two and three dimensions. In two dimensions, the lowest two non-trivial frequencies are nearly degenerate, and in three dimensions triply degenerate, as expected from the analysis of eigenmodes in an ordered-lattice geometry. Looking at higher non-trivial frequencies, their values are consistent with the coarse-grained ordered picture, predicting particular ratios of the low lying frequencies, as shown in Table 1.

The average spatial profile of these low frequency modes clearly shows plane wave oscillations, as shown in Fig. 1.

DETAILS OF THE RECURSIVE GREEN FUNCTION CALCULATIONS.

The recursive Green function technique with finite size scaling was first used to study Anderson localization by MacKinnon and Kramer [6]. It studies quasi-one-dimensional systems with one very long axis and $d-1$ shorter axes, of width w. The system is built recursively by stitching together many $(d-1)$-dimensional strips. In the original Anderson model, each site is coupled only to its nearest neighbors, so each new slice has direct couplings only to the closest neighbors; this property is essential for the recursion.

In Ref. 7, we extended this technique to non-lattice problems, as studied in this paper. Without a lattice, the quasi-one-dimensional system is stitched together from slices of width w and length l, which contain a random number of sites, chosen from a Poisson distribution with a mean density ϵ^d. In order to have particles in each slice interact only with particles in the nearest neighbor slices, we must impose a cutoff on the interaction between sites.
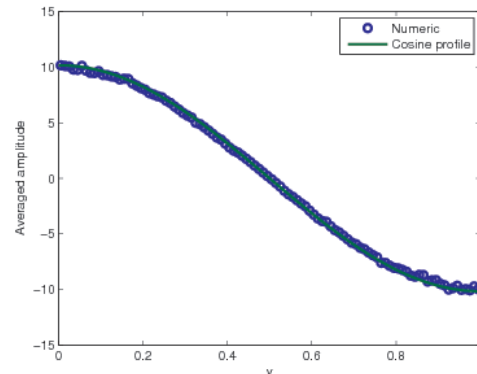

FIG. 1. The lowest frequency mode is shown for a single matrix with $N = 500,000$, in two dimensions, with $\epsilon = 0.1$. The amplitudes were binned along one of the sides of the square in which the points are randomly chosen, and the graph shows the sum of amplitudes in each bin. While the eigenmode itself is not a simple plane wave, after 'coarse-graining' in this way one obtain a cosine profile, precisely as would be obtained in an ordered system.
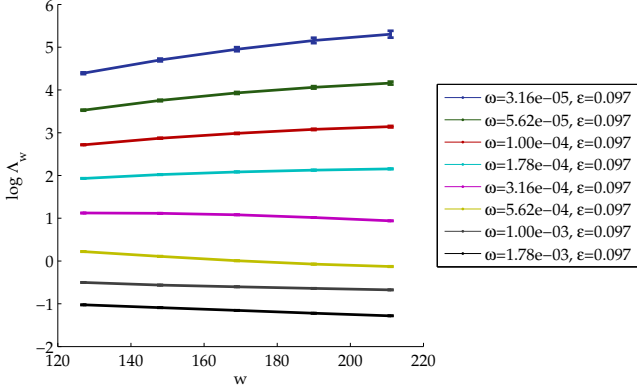
FIG. 2. Part of the data used to produce the phase diagram in Figure 2 of the main text. For $\epsilon = 0.097$ in $d = 2$, we show $\Lambda_w(w)$. The phase boundary between the localized (sloping down) and delocalized (sloping up) energies is clear.

That is, we set $\exp(-r) \to 0$ for $r \geq L_c$ for some cutoff L_c. Since we use periodic boundary conditions in the $d - 1$ dimensions of the slice, we choose the cutoff to be $L_c = \min[l, w/2]$. Since there is no lattice, w and l must be chosen appropriately large so that the system is not disconnected.

We begin with a single slice of width w and length l. We add a second slice and find the portion of the energy-resolved Green function $G(\lambda)$ that connects any site in slice 1 to any site in slice 2. We recursively add more sites, always finding the portion of G connecting sites in slice 1 to sites in slice N, $G_{1N}^N(\lambda) = \langle 1|G^N(\lambda)|N\rangle$. $G_{1N}^N(\lambda)$ is an $M_1 \times M_N$ matrix, where M_i is the number of sites in slice i. The probability for a particle injected with energy λ into slice 1 to make it to any site in slice N is

$$P_N = \text{Tr}[G_{1N}^N(\lambda)]^{1/2}. \tag{5}$$

Since all states are localized in 1d systems, P_N decays like $\exp(-2Nl/\ell_w)$, for localization length ℓ_w. We extract the effective localization length at energy λ and width w by

$$\frac{2}{\ell_w} = -\lim_{N\to\infty} \frac{\log P_N}{Nl}. \tag{6}$$

N must be chosen large enough to get good statistical accuracy for ℓ_w [8, 9]. Statistically, the system behaves as though it consists of Nl/ℓ_w independent and identically distributed samples chosen from a normal distribution, so the sampling error decreases as $N^{-1/2}$.

When ℓ_w has been acquired for a range of widths w, the theory of single-parameter scaling is used to extrapolate to the infinite-size system [6, 9, 10]. According to single-parameter scaling, for sufficiently large w that irrelevant corrections can be neglected, the dimensionless scaling variable $\Lambda_w \equiv \ell_w/w$ obeys a universal scaling law

$$\Lambda_w = F\left[\frac{\phi(\epsilon, \lambda)}{w}\right] \tag{7}$$

for some unknown universal function F, where $\phi(\epsilon, \lambda)$ characterizes the infinite-size system: it is the localization length for localized systems and the correlation length for delocalized systems. In particular, if Λ_w increases with w, then the state is delocalized and if Λ_w decreases with w, then the state is localized. This is the approach adopted to determine the phase diagram in Figure 3 of the main text. Single-parameter scaling has been demonstrated to hold in similar systems without the sum rule [7], but it has not yet been proved in this system. It is possible that the emergence of the percolation length l^* would cause a breakdown in the single-parameter scaling, but the data so far do not show any such signs.

The details of setting up the recursive Green function calculation have been extensively given elsewhere [11, 12]. The basic principle is that, in each step, the exact Green function of the wire with N slices G^N and the exact Green function of the new slice g are known. We write $G_0 = G^N + g$. The perturbation that connects them V can be treated non-perturbatively using a Dyson equation

$$G^{N+1} = G_0 + G^{N+1}VG_0 = G_0 + G_0VG^{N+1}. \tag{8}$$

Matrix elements taken on Eq. 8 give the recursion relations required.

For our case, the sum rule in the definition of the matrix K means that the perturbation V contains not only off-diagonal terms connecting sites in the two slices, but also contains diagonal terms, adjusting the on-site energy of each site. This does not pose any difficulty for the method, but requires more matrix operations per calculation, increasing the cost of the calculation.

In each calculation, we choose the values of λ we wish to study, and for each λ store the matrices G_{1N}^N, G_{11}^N and G_{NN}^N. For the $N+1$st slice being added to the system, it has a Hamiltonian K and the off-diagonal perturbation connecting the existing wire to the new slice is U. Then in the usual problem, without the sum rule, the result is

$$G_{N+1,N+1}^{N+1} = (\lambda - K - U^\dagger G_{N,N}^N U)^{-1}, \tag{9}$$

$$G_{1,N+1}^{N+1} = G_{1,N}UG_{N+1,N+1}^{N+1}, \tag{10}$$

$$G_{1,1}^{N+1} = G_{1,1}^N + G_{1,N}^N U(G_{1,N}^{N+1})^\dagger, \tag{11}$$

where we used $g^{-1} = \lambda - K$. When we include the sum rule, the perturbation contains the off-diagonal terms U, the diagonal terms U_N acting on the sites in the Nth slice, and the diagonal terms U_{N+1} acting on the sites of the new slice. Then we find

$$G_{N+1,N+1}^{N+1} = [\lambda - K - U^\dagger(\mathbb{1}_{M_N} - G_{N,N}^N U_N)^{-1} G_{N,N}^N U - U_{N+1}]^{-1}, \tag{12}$$

$$G_{1,N+1}^{N+1} = G_{1,N}^N[\mathbb{1}_{M_N} + U_N(\mathbb{1}_{M_N} - G_{N,N}^N U_N)^{-1} G_{N,N}^N]U G_{N+1,N+1}^{N+1}, \tag{13}$$

$$G_{1,1}^{N+1} = G_{1,1}^N + \left\{ G_{1,N}^N U(G_{1,N}^N)^\dagger + G_{1,N}^N U_N(\mathbb{1}_{M_N} - G_{N,N}^N U_N)^{-1}[(G_{1,N}^N)^\dagger + G_{N,N}^N U(G_{1,N+1}^{N+1})^\dagger] \right\}. \tag{14}$$

If the calculations are done all at once, there is no need to store $G_{1,1}$. But it is often convenient to break the calculation of a very long wire into many smaller pieces, and then stitch them together. This stitching requires that $G_{1,1}$ be stored. Consider one wire with N_1 slices with recursively calculated Green functions $G_{1,1}^{N_1}$, $G_{1,N_1}^{N_1}$, and $G_{N_1,N_1}^{N_1}$ and a second wire with N_2 slices with recursively calculated Green functions $g_{1,1}^{N_2}$, $g_{1,N_2}^{N_2}$, and $g_{N_2,N_2}^{N_2}$. Let $N = N_1 + N_2$. Then we can stitch g onto G to find

$$G_{N,N}^N = g_{N_2,N_2}^{N_2} + G_{N_1+1,N_2}^N U g_{1,N_2}^{N_2} + \left\{ (g_{1,N_2}^{N_2})^\dagger + G_{N_1+1,N_2}^N U g_{1,1}^{N_2})[\mathbb{1}_{M_{N_1}} - U_{N+1}g_{1,1}^{N_2}]^{-1} U_{N+1}g_{1,N_2}^{N_2} \right\}, \tag{15}$$

$$G_{N_1+1,N_2}^N = g_{1,N_2}^{N_2}[\mathbb{1}_{N+1} - U_{N+1}g_{1,1}^{N_2}]^{-1} U^\dagger G_{N_1,N_1}^{N_1} D, \tag{16}$$

$$D = [\mathbb{1}_{M_{N_1}} - U g_{1,1}^{N_2}(\mathbb{1}_{M_{N_1+1}} - U_{N+1}g_{1,1}^{N_2})^{-1} U^\dagger G_{N_1,N_1}^{N_1} - U_{N_1} G_{N_1,N_1}^{N_1}]^{-1}, \tag{17}$$

$$G_{1,N}^N = G_{1,N_1}^{N_1} D U \left\{ \mathbb{1}_{M_{N_1}} + g_{1,1}^{N_2}[\mathbb{1}_{M_{N_1}} - U_{N+1}g_{1,1}^{N_2}]^{-1} U_{N_1} \right\} g_{1,N_2}^{N_2}, \tag{18}$$

$$G_{1,1}^N = G_{1,1}^{N_1} + G_{1,N_1}^{N_1} D \left\{ U g_{1,1}^{N_2}[\mathbb{1}_{M_{N_1}} - U_{N+1}g_{1,1}^{N_2}]^{-1} U^\dagger + U_{N_1} \right\} G_{1,N_1}^{N_1}. \tag{19}$$

It is generally desirable to let N be large enough that the statistical error in ℓ_w is less than 1%. For values of λ, ϵ where the states are highly delocalized, ℓ_w can be very long, requiring an inordinate length N to get reasonable errors. Conveniently, the values of ℓ_w are reasonable for the localized states and the nearby delocalized points, so we can extract the delocalization boundary $\omega^*(\epsilon)$, while we cannot quite prove that the strongly delocalized states are actually delocalized. Care must be taken to avoid both overflow and underflow in storing $G_{1,N}$, as detailed in Ref. [12].

Figure 2 shows some of the calculations used to create Figure 2 of the main text. The statistical error bars are smaller than the data points for all but the lowest energy (most delocalized) state. For these simulations, $l = 50$ and N ranged from $2 \cdot 10^5$ to $2.6 \cdot 10^7$.

[2] S. Tyč and B. I. Halperin, Phys. Rev. B **39**, 877 (1989).

[3] A. Amir, Y. Oreg, and Y. Imry, Phys. Rev. Lett. **105**, 070601 (2010).

[4] V. Ambegaokar, B. I. Halperin, and J. S. Langer, Phys. Rev. B **4**, 2612 (1971).

[5] I. Lifshitz, Advances in Physics **13**, 483 (1964).

[6] A. MacKinnon and B. Kramer, Phys. Rev. Lett. **47**, 1546 (1981).

[7] J. J. Krich and A. Aspuru-Guzik, Phys. Rev. Lett. **106**, 156405 (2011).

[8] K. Slevin and T. Ohtsuki, Phys. Rev. Lett. **82**, 382 (1999).

[9] P. Markos, Acta Physica Slovaca **56**, 561 (2006).

[10] E. Abrahams, P. W. Anderson, D. C. Licciardello, and T. V. Ramakrishnan, Phys. Rev. Lett. **42**, 673 (1979).

[11] H. U. Baranger, D. P. DiVincenzo, R. A. Jalabert, and A. D. Stone, Phys. Rev. B **44**, 10637 (1991).

[12] A. MacKinnon and B. Kramer, Z. Phys. B **53**, 1 (1983).

[1] P. L. Doussal, Phys. Rev. B **39**, 881 (1989).